Journal of Materials Chemistry A

PAPER

View Article Online
View Journal | View Issue



Cite this: J. Mater. Chem. A, 2015, 3, 18083

# Photocatalytic activity of ZnO/$GaP_{1-x}N_x$ for water splitting†

Chihiro Oshima,[a] Hiroshi Nishiyama,[b] Abhijit Chatterjee,[c] Katsunori Uchida,[d] Kazunori Sato,[d] Yasunobu Inoue,*[a] Takashi Hisatomi[e] and Kazunari Domen[e]

Received 26th June 2015
Accepted 28th July 2015

DOI: 10.1039/c5ta04732c

www.rsc.org/MaterialsA

The phosphidation of a ZnO/GaN solid solution photocatalyst enhanced significantly its activity for water splitting. The photocatalysts were heated with phosphorus in a vacuum-sealed quartz tube. Activation due to phosphidation was restricted within the narrow temperature range of 823–873 K, and varying amounts of P were added to the solid solution. In addition to X-ray diffraction peaks due to ZnO/GaN, active phosphide ZnO/GaN provided a single GaP peak with diffraction angles higher than normal GaP by $2\theta = 0.20–0.44°$, indicative of the formation of a $GaP_{1-x}N_x$ alloy system. The diffraction peaks were simulated using first principles Ab inito calculations on molecular models of $Ga_{32}P_{32-y}N_y$. The comparison with experimental shifts showed that the highest activity was induced in an $x$ range of 0.034–0.074 of $GaP_{1-x}N_x$.

## Introduction

New visible-light activated photocatalysts for water splitting have been an important development. Among $d^{10}$ electron configuration photocatalysts consisting of typical elements, GaN is one of the promising candidates. Doping of divalent ions, such as $Mg^{2+}$, $Zn^{2+}$, $Be^{2+}$, into GaN to form p-type GaN, converted GaN into a photocatalyst that was active for water splitting to produce $H_2$ and $O_2$ when combined with a $RuO_2$ cocatalyst.[1,2] The band most useful for the reaction of GaN was limited to wavelengths shorter than 380 nm. To extend absorption to the visible light region, a solid solution of ZnO and GaN, ZnO/GaN, has promoted water splitting in the visible light region of 530 nm when combined with co-catalysts such as $RuO_2$ and $Cr_2O_3$-coated Rh metal.[3–10]

GaP is a $d^{10}$ phosphide. The band gap of this material is approximately 2.25 eV at 300 K and the threshold of light absorption is approximately 560 nm. However, there have so far been a few reports on its application as a photocatalyst for water splitting. One disadvantage is for photoexcitation, in which the transition of photon-induced electrons from the valence to the conduction band is indirect. Many reports have shown that incorporating small amounts of N into GaP induces a change in the fundamental optical transition from an indirect-gap ($\Gamma_{15} - X_1$) transition of GaP[11,12] to a direct-gap transition and lowering the band gap with increasing N concentration.[13–27] The N-induced decrease in the band gap is a result of an interaction between the nitrogen atoms and the GaP matrix, which forms a $GaP_{1-x}N_x$ alloy system.[16–19,22] These results indicate that $GaP_{1-x}N_x$ compounds, or at least $GaP_{1-x}N_x$ layer formation on either GaN or GaP, efficiently produce visible-light driven photoexcited carriers, and thus it is of interest to apply the $GaP_{1-x}N_x$ system as a photocatalyst for water splitting. Previously, $GaP_{1-x}N_x$ ($x$ = 0–0.035) was grown using a metal organic chemical vapor deposition (MOCVD) technique on GaP and then employed as an electrode for water-splitting reactions. The band edges were shown to be too negative to drive water-splitting, although the $GaP_{0.98}N_{0.02}$/GaP had a band gap of ~2 eV optimal for water splitting applications.[28] However, photocatalysis of $GaP_{1-x}N_x$ for water splitting is still ambiguous, because of its electronic properties sensitive to P and N compositions, and thus it has to be examined from the viewpoint of the introduction of a small amount of nitrogen atoms that is a key to obtain the active $GaP_{1-x}N_x$ alloy system.

There are two ways to prepare Ga–N–P-compounds. The nitridation of GaP has mostly been used. Another strategy, which is scarcely examined, is phosphiding the GaN surface. The present study describes the results of GaP nitridation and GaN phosphidation, which revealed that the latter using ZnO/GaN produced highly active photocatalysts for the water splitting reaction. The photocatalytically active $GaP_{1-x}N_x$ structures

[a]Department of Materials Science and Technology, Nagaoka University of Technology, Nagaoka 940-2188, Japan. E-mail: inoue@analysis.nagaokaut.ac.jp; yasinoue@chemsys.t.u-tokyo.ac.jp

[b]Department of Chemical System Engineering, School of Engineering, The University of Tokyo, 5-1-5 Kashiwahara, Kashiwa, Chiba, 277-8589 Japan

[c]Dassault Systemes Biovia K.K., ThinkPark Tower 21F, 2-1-1 Osaki, Shinagawa-ku, Tokyo 141-6020, Japan

[d]Department of Environmental Engineering, Nagaoka University of Technology, Nagaoka 940-2188, Japan

[e]Department of Chemical System Engineering, School of Engineering, The University of Tokyo, Tokyo 113-8656, Japan

† Electronic supplementary information (ESI) available: Full description of the material. See DOI: 10.1039/c5ta04732c

are discussed based on cluster simulation for a new GaP phase produced by phosphidation.

## Experimental section

A solid solution of ZnO/GaN, that is $(Ga_xZn_{1-x})(N_xO_{1-x})$, was prepared by nitriding metal oxides under a $NH_3$ flow according to a method reported previously.[1–6] The starting material was a powder containing 1 : 2 molar ratio of $Ga_2O_3$ (99.98% pure reagent from Nacalai Chemical Co. Ltd) and ZnO (extra grade from Nacalai Chemical Co. Ltd), which was mixed in an agate mortar and placed in a quartz tube. The quartz tube was set in a rotary kiln furnace, where the powder was slowly rotated to undergo uniform nitridation with gaseous $NH_3$. The flow rate of $NH_3$ was 300–400 mL $min^{-1}$. The nitridation temperature and time were 1123 K and 14 h, respectively. For phosphidation, the ZnO/GaN prepared was mixed with red phosphorus (99.9%; Aldrich) in a quartz tube, sealed under vacuum, and then heated at temperatures from 773 to 1073 K. The phosphidation time was 7–28 h. The ratio of P to ZnO/GaN in the sealed quartz tube is an important factor for phosphidation, therefore the molar ratio of P to ZnO/GaN was adjusted from 0 to 0.10. The ZnO/GaN prepared by phosphidation is referred to as ZnO/GaN-P ($T$, $R$) for simplicity, where $T$ and $R$ represent the temperature and molar ratio of P to ZnO/GaN upon phosphidation, respectively. For example, ZnO/GaN-P (823, 0.07) indicates phosphidation at 823 K using a molar ratio of 0.07.

For the preparation of $GaP_{1-x}N_x$ photocatalysts, GaP (99.999%; Kojundo Chemicals Co. Ltd) was nitrided for 3–16 h between 873 and 1123 K at an $NH_3$ flow rate of 300 mL $min^{-1}$. In addition, ZnO was added at a molar ratio of 0.5–5% to GaP and then subjected to a similar nitridation process.

For the loading of $RuO_2$ as a cocatalyst, the nitrides and phosphides prepared were dispersed in THF containing the Ru carbonyl complex $Ru_3(CO)_{12}$ at room temperature, dried under vacuum, and then oxidized at 623 K for 1.5 h to convert the complex to $RuO_2$ particles.[1,2] The loading of the cocatalyst was 3.5 wt% based on the amount of Ru metal. A 3.5 wt% $RuO_2$-loaded ZnO/GaN photocatalyst was denoted as $RuO_2$–ZnO/GaN, unless otherwise specified.

Water splitting was conducted in a closed gas-circulating apparatus equipped with a Pyrex glass reactor and gas chromatograph for analyzing $H_2$ and $O_2$ gas, as described elsewhere.[1,2] The photocatalyst powder (0.2 g) was dispersed in ion-exchanged water using a magnetic stirrer followed by irradiation of incident light intensity (50 mW $cm^{-2}$) using a 300 W Xe lamp (Eagle Engineering LX300) from the outside. The reactor was cooled to 293 K by water circulating through a water jacket during the photocatalytic reaction.

In the simulation of XRD peak patterns, we have used a supercell of 2 × 4 × 1 for a 64 atom structure with the composition $Ga_{32}P_{32}$. The model was chosen to give a symmetric substitution for the dopant nitrogen. The central strand was taken to minimize the interaction of the dopant arising from periodic boundary consideration. All the calculations were performed using the CASTEP (Cambridge Serial Total Energy Package) and the associated programs for symmetry analysis, which has been described elsewhere.[29–31] CASTEP is a pseudopotential total energy code that employs Perdew and Zunger[32] parameterization of the exchange-correlation energy, super cells and special point integration over the Brillouin zone and a plane wave basis set for the expansion of wave functions. Becke–Perdew parameterization of the exchange-correlation functional, which includes gradient correction (GGA),[33,34] was employed. The pseudopotentials are constructed from the CASTEP database. Reciprocal space integration over the Brillouin zone is approximated through careful sampling at a finite number of $k$ points using the Monkhorst-Pack scheme.[35] Here we used symmetric 5 $k$-points in all calculations. The basis cutoff used is 300.0 eV. The energy tolerance is $1.0 \times 10^{-5}$ eV per atom, the force tolerance 0.3 eV $nm^{-1}$, maximum stress 0.05 GPa and the displacement tolerance 0.0001 nm.

## Results

The X-ray diffraction patterns of GaP nitrided between 873 and 1123 K consisted of strong GaP peaks, and no significant peak shifts were observed (ESI, Fig. S1†). Very small peaks attributed to GaN appeared. For $RuO_2$-loading on the nitrided GaP, there was no significant production of $H_2$ and $O_2$, although a very small amount of $H_2$ production occurred. In nitridation of a ZnO and GaP mixture, X-ray diffraction patterns were nearly the same as those of GaP, and slight photocatalytic activity for $H_2$ production was found, but no oxygen evolution was observed. The procedure for obtaining $GaP_{1-x}N_x$ by nitriding GaP and a mixture of ZnO and GaP failed to produce active photocatalysts.

Fig. 1 shows results of water splitting using $RuO_2$–ZnO/GaN and $RuO_2$–ZnO/GaN-P (823, 0.07), respectively. No gas-phase products were observed for either photocatalyst without light irradiation. For $RuO_2$–ZnO/GaN, light irradiation resulted in the immediate production of both $H_2$ and $O_2$, which was nearly proportional to the irradiation time. Re-running the reaction after evacuating the gas-phase products resulted in a similar production of $H_2$ and $O_2$. Even after the fourth run, gas production occurred steadily. The production ratio of $H_2$ to $O_2$ was 2.1 : 1. For $RuO_2$–ZnO/GaN-P (823, 0.07), both $H_2$ and $O_2$ evolved immediately upon light irradiation, with the initial photocatalytic activity nearly 8-fold greater than that of original $RuO_2$–ZnO/GaN. Upon repeating the photocatalytic reaction, production gradually was reduced, and became constant after the third repeat. Interestingly, this production was still nearly 6-fold greater than that using $RuO_2$–ZnO/GaN. The production ratio of $H_2$ to $O_2$ was 2.2 : 1.0.

The effects of phosphidation on the catalytic activity of $RuO_2$–ZnO/GaN were examined in the temperature range of 823–1073 K at different molar ratios of ZnO/GaN to P. The photocatalytic activity of $RuO_2$–ZnO/GaN-P (773, 0.1) was too low to detect. Fig. 2 shows the results using $RuO_2$–ZnO/GaN-P (823, $x$) with $x = 0$–0.1. The activity increased with the value of $x$, reached a maximum at $x = 0.07$, and then decreased slightly. In $RuO_2$–ZnO/GaN-P (873, $x$) at $x$ = 0–0.10, the activity was enhanced as the value of $x$ increased, passed through a maximum at $x$ = 0.05, and then decreased significantly. The maximum activity frequently occurred when phosphidation was

 

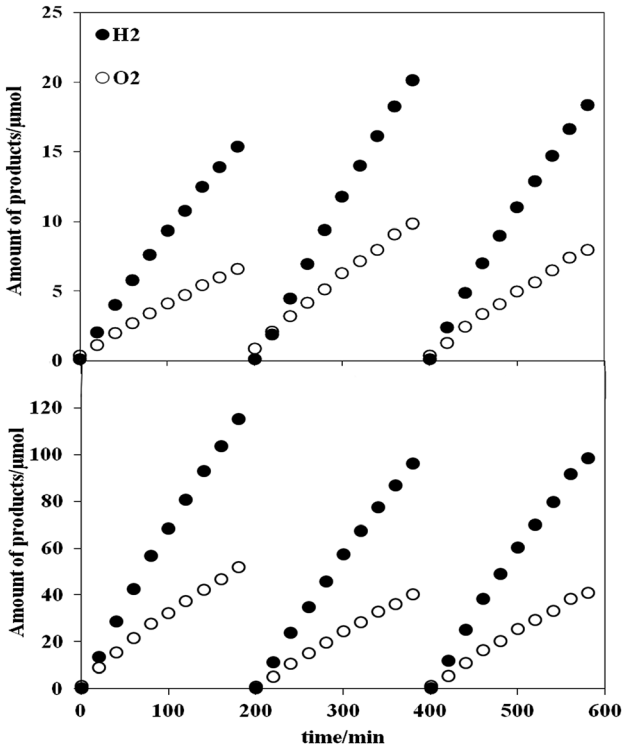


Fig. 1 Evolution of $H_2$ and $O_2$ during water splitting by untreated ZnO/GaN (upper) and ZnO/GaN-P (823, 0.07) (lower). Filled circle: $H_2$, open circle: $O_2$.

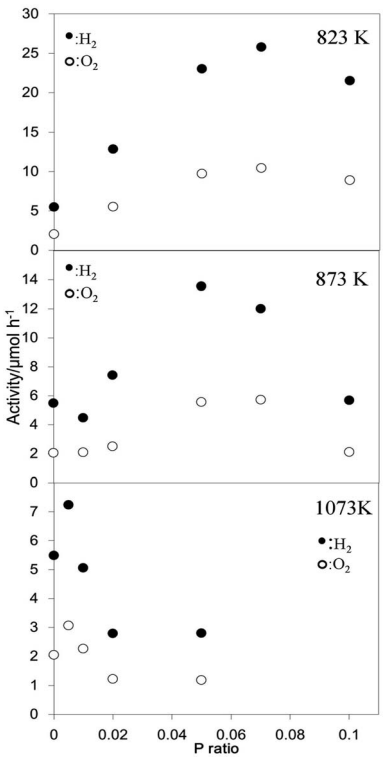


Fig. 2 Changes in the photocatalytic activity as a function of the molar ratio of P at temperatures of 823 (upper), 873 (middle), and 1073 K (lower). Filled circle: $H_2$, open circle; $O_2$.

conducted between 823 and 873 K, although the P ratio at the maximum was different. The results using $RuO_2$–ZnO/GaN-P (1073, $x$) with $x = 0$–0.05 showed that the activity increased at $x = 0.005$, followed by a monotonous decrease with increasing $x$. It is to be noted that no activation occurred when ZnO/GaN was heated under similar conditions in a vacuum-sealed quartz tube without phosphorus.

Fig. 3 shows the effects of time on ZnO/GaN upon phosphidation at 823 K. Phosphidation for 7 h resulted in little activation, with activity nearly the same as the original ZnO/GaN. A sharp increase in activity occurred upon phosphidation for 14 h, followed by the appearance of a maximum at 21 h, and then a slight decrease for 28 h. Note that the phosphidation of ZnO/GaN led to the formation of photocatalysts with significantly greater activity than the original ZnO/GaN when $RuO_2$ was loaded as the cocatalyst. The phosphidation temperatures suitable for high activity generation remained in the narrow range of 823–873 K. The SEM observation showed that there were no significant changes in the morphology of ZnO/GaN particles and their aggregates by phosphidation (ESI Fig. S2†). Thus, the activity enhancement is not directly associated with crystal growth of specific planes but the effect of N and P atom combination.

Fig. 4 shows the UV-Vis diffuse reflectance spectrum of ZnO/GaN-P (823, 0.07), together with ZnO/GaN. Light absorption started at around 500 nm, then increased sharply and reached a maximum at approximately 350 nm. A shift to a shorter wavelength by ~7 nm was observed in comparison with ZnO/GaN.

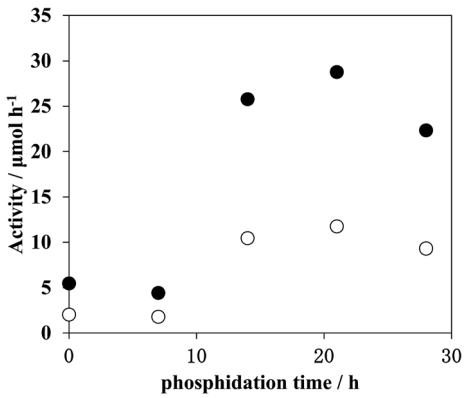


Fig. 3 Changes in the photocatalytic activity with phosphidation time during the preparation of ZnO/GaN-P (823, 0.07). Filled circle: $H_2$, open circle: $O_2$.

Fig. 5 shows X-ray diffraction patterns of ZnO/GaN-P (823, 0.07) and ZnO/GaN. The patterns were characteristic of a wurtzitic structure, and despite the phosphidation temperature, time, and varying P amounts, strong peaks attributed to ZnO/GaN always were observed. No shifts or broadening of the main peaks attributed to GaN occurred. Neither $ZnP_2$ nor $Zn_3P_2$ peaks were observed. Both ZnO/GaN-P (823, 0.07) and untreated ZnO/GaN exhibited nearly the same peak patterns except for the appearance of a small peak near $2\theta = 28°$ for ZnO/GaN-P (823, 0.07). This peak was originally due to GaP, but is different in

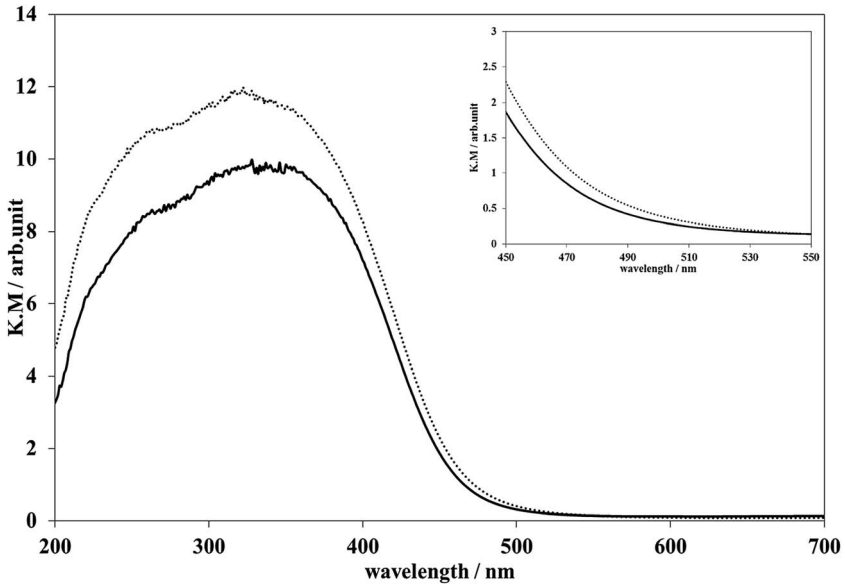


Fig. 4 UV-Vis diffuse reflectance spectra of untreated ZnO/GaN (dash line) and ZnO/GaN-P (823, 0.07) (solid line). Inset figure shows the detail in the range of 450–550 nm.

peak position from the original GaP. These results indicate that phosphidation producing GaP takes place in surface regions, and the interior remains as GaN. Fig. 6 shows the X-ray diffraction patterns of the $2\theta = 28$–$29^\circ$ region for ZnO/GaN-P (873, $x$) as a function of $x$. Below $x = 0.01$, no significant diffraction peaks were observed in this region. A single peak appeared at $2\theta = 28.50^\circ$ for $x = 0.05$, which shifted to $2\theta = 28.68^\circ$ for $x = 0.07$. For $x = 0.1$, two peaks appeared at $2\theta = 28.32^\circ$ and $2\theta = 28.68^\circ$. The peak shifts of GaP to a higher angle indicates that the N atoms are involved in a fundamental unit of the tetrahedral $GaP_4$, producing $GaP_{1-x}N_x$, because the $N^{3-}$ size is smaller than that of $P^{3-}$. Therefore, the shift of the GaP diffraction peak represents a change in the active site conformation induced by P introduction.

Fig. 7 shows the X-ray diffraction patterns of ZnO/GaN-P (823, 0.07) at different phosphidation times. A single peak appeared at $2\theta = 28.62^\circ$ upon heating for 7 h. The peak increased in size at 14 h, and shifted slightly to a lower diffraction angle by $0.07^\circ$ at 21 h. A very slight shift to a lower diffraction angle occurred with 28 h of phosphidation. To

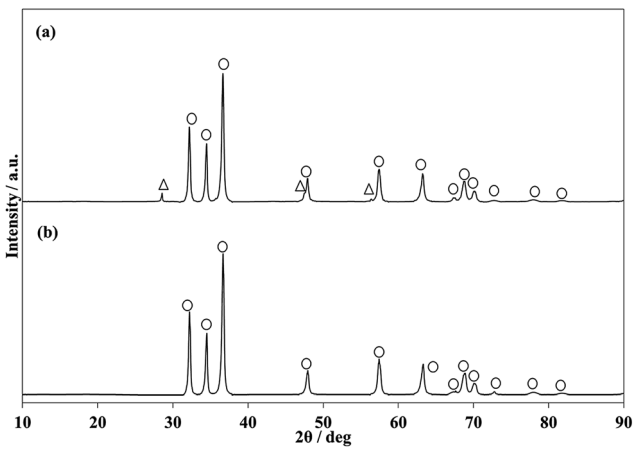


Fig. 5 X-ray diffraction patterns of untreated ZnO/GaN (lower) and ZnO/GaN-P (823, 0.07) (upper). Open circles and triangles show diffraction peaks due to ZnO/GaN and GaP, respectively.

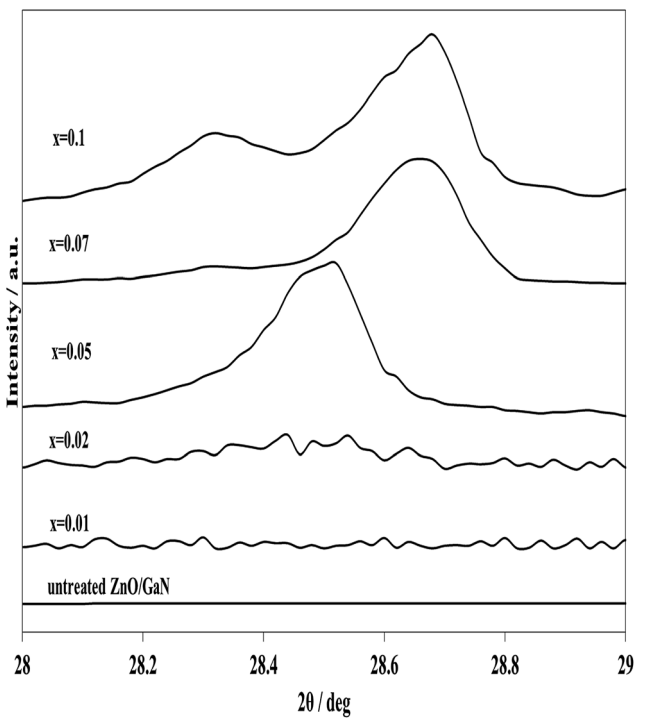


Fig. 6 X-ray diffraction patterns in the range of $2\theta = 28$–$29^\circ$ for ZnO/GaN-P (873, $x$) with an $x$ value in the range of 0.01 to 0.1 and untreated ZnO/GaN.

visualize the active structures, the photocatalytic activity obtained under various conditions such as different phosphidation temperatures, time and P amounts was consolidated and plotted against diffraction peak positions due to GaP in the range $2\theta = 28$–$29^\circ$. As shown in Fig. 8, the photocatalytic activity at 823 K increased as the diffraction angle increased from $2\theta = 28.32^\circ$ (GaP crystal), producing a maximum at approximately $2\theta = 28.6^\circ$, and decreases with further increase in the diffraction angle. A similar trend can be seen for 873 K phosphidation.

These correlations demonstrate that a high photocatalytic activity depends on the structures of $GaP_{1-x}N_x$ formed through the gas–solid reaction between vaporized P and GaN. To determine the active conformation, the diffraction peak shifts were simulated by taking the geometry optimized model of the $Ga_nP_{n-y}N_y$ into account. Fig. 9 shows the GaP diffraction peaks calculated by the powder diffraction method as implemented in the Reflex Module of the Dassault Systemes BIOVIA method for $n = 32$ and $y = 1, 3, 4, 6, 7$ and 8. A $2\theta$ range of 10 to $90^\circ$ was used with a step size of 0.05. Peak position errors can result from an incorrect zero point or from errors in the placement or transparency of the sample. In this case we have used Bragg–Brentano correction.[36] A peak due to $Ga_{32}P_{32}$ appeared at $2\theta = 27.65^\circ$, shifted to a higher angle with increasing N atom content, and attained at $2\theta = 28.44^\circ$ for $y = 4$, $2\theta = 28.75^\circ$ for $y = 6$ and $2\theta = 29.03^\circ$ for $y = 8$. The diffraction angle shifts against the percentage of P atoms in the total of P and N atoms P/(P + N) × 100% showed a good linear relationship (ESI Fig. S3†). In comparison with the experimental value which provides the greatest photocatalytic activity for shifts by $2\theta = 0.20$–$0.44^\circ$ to a higher diffraction angle from GaP (Fig. 8), the linear relationship provided the result that the optimal conditions for the highest activity are the involvement of N at the percentage of 3.4–7.4% in GaP.

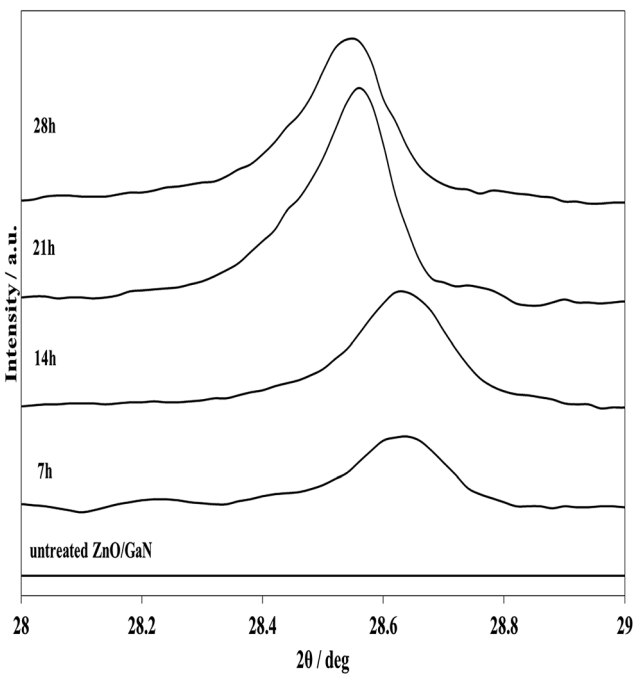


Fig. 7 X-ray diffraction patterns in the range of $2\theta = 28$–$29^\circ$ for ZnO/GaN-P (823, 0.07) at different phosphidation times from 7 to 28 h and untreated ZnO/GaN.

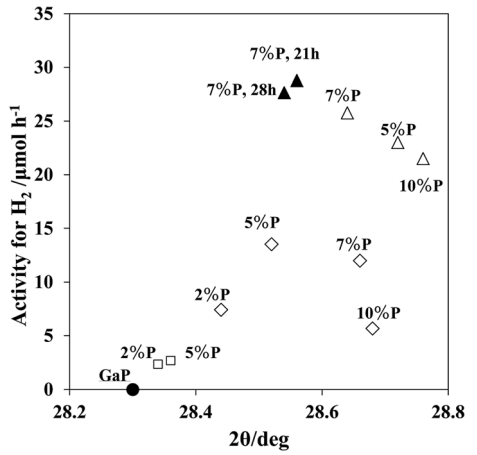


Fig. 8 Photocatalytic activity *vs.* diffraction peak angles of GaP produced by phosphidation. The diffraction peak angle of normal GaP is shown for comparison. The photocatalytic activity for $H_2$ production only was shown for simplicity. Numbers in figure shows the molar percentage of P added to ZnO/GaN and the time for phosphidation. No expression of time means 14 h phosphidation. Open and filled triangles: ZnO/GaN phosphidated at 823 K. Open rhombus: at 873 K. Open square: at 1073 K. Filled circle: normal GaP.

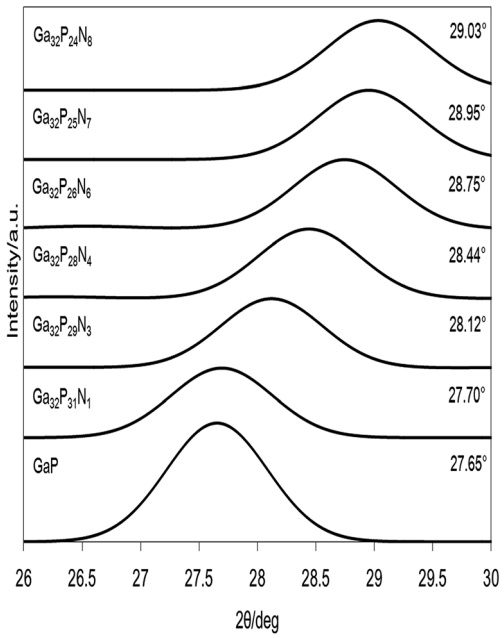


Fig. 9 Simulated X-ray diffraction peaks of GaP for $Ga_{32}P_{32-y}N_y$ ($y = 1$–8).

In order to see the electronic contribution of N atom in GaP, the density of states (DOS) was calculated by a DFT method assuming a super cell of $Ga_{32}P_{31}N_1$ (the inclusion of the ZnO component caused a complexity in calculation, and its contribution is ignored here). Fig. 10 shows the total DOS and atom orbital (AO)-projected DOS (AO-PDOS). The occupied bands appearing with increasing energy consist of a sharp Ga 3d AO at

around −14 eV, P 3s AO at around −10 eV, and the valence band, in which the lower energy part is mainly due to Ga 4s + P 3p + N 2p orbitals. The HOMO is composed of Ga 4p + P 3p + N 2p AOs. In the unoccupied bands, LUMO consists of Ga 4s4p + P 3p + N 2s AOs. The band gap is estimated to be 0.793 eV.

## Discussion

The phosphidation of ZnO/GaN increased the photocatalytic activity for water splitting by a factor of 6–8. The quantum efficiency was estimated to be in the range 1–2% from comparison with photocatalytic activity previously obtained for $RuO_2$–ZnO/GaN without phosphidation.[4,5] The phosphidation conditions are restricted in a very narrow range in temperatures and the P amounts introduced, which indicates that the activation is very sensitive to the ratio of P to N. The appearance of new GaP peaks with higher X-ray diffraction angles, different from GaP crystal, is apparently associated with the photocatalyst activation. No shifts of GaP diffraction peaks in the inactive nitrided GaP (ESI Fig. S1†) are in line with this view. The simulation for the relationship of N contents *vs.* diffraction shifts (ESI Fig. S3†) showed that the high photocatalyst activation occurred at 3.4–7.4% of N concentrations in GaP. It should be noted that a small amount of N atoms in GaP is effective for the activation of GaP surfaces.

GaP and GaN have a zinc blende and wurtzite structure, respectively. The differences in the crystal structures and lattice constant (~20%) produce a large miscibility gap.[37] Thus, in the growth of $GaP_{1-x}N_x$ alloys, the N concentration was usually restricted below $1 \times 10^{19}$ $cm^{-3}$ or 0.04%, but recently it was increased to as high as 3.1–7.6% in $GaP_{1-x}N_x$ films epitaxially grown by MOVPE[16] and molecular beam epitaxy (MBE).[17–20,22] The introduction of N in GaP is a heavy isoelectric doping that has band effects. Photoluminescence (PL) measurements[16–19,22] and theoretical calculations[23–27] showed that the very limited N concentration of $<10^{17}$ $cm^{-3}$ produced an A-line due to the isolated N atom, and in the N concentration increasing up to $\sim 10^{19}$ $cm^{-3}$, different $NN_i$ ($i < 10$) pairs were formed below the band gap. The concentration is not enough to change the potential of the band edge. However, the $NN_i$ pairs produce isoelectronic traps in the band and bind the electrons,[13] which might be useful for photoexcited charge separation. At a higher N concentration of >0.5%, a band formed by N atoms merged the conduction band edges of GaP. Thus, the N atom concentration obtained in the present study is considered to contribute to the conduction band formation. This is confirmed from the DOS calculation for a model of $Ga_{32}P_{31}N_1$ (3.1% N) that provided the conduction bands of hybridized Ga 4s4p + P 3p + N 2s AOs.

A maximum was observed in the relationship of photocatalytic activity against GaP peak shifts (Fig. 8). As phosphidation progressed, larger shifts of the GaP diffraction peak occurred, and also the diffraction peak assigned to the original GaP crystal appeared, as shown in Fig. 6. Thus, the photocatalytic activity that decreases with larger diffraction peak shifts are due to not only the dilution of N atom concentrations but the formation of inactive GaP phases.

The UV-Vis diffuse reflectance spectrum showed that the light absorbing wavelength of ZnO/GaN-P was slightly (~7 nm) shorter than that of ZnO/GaN, opposite to those reported for the formation of the $GaP_{1-x}N_x$ phase, in which the N atom inclusion in GaP caused shifts to a longer wavelength. The present ZnO/GaN system had characteristics of absorbing longer wavelength light than GaN, because of the solid solution effects of ZnO.[10,38] It seems likely that the partial removal of the ZnO component from ZnO/GaN surfaces during phosphidation in vacuum has larger effects than the phosphidation, which results in the light absorption edge shifts to shorter wavelengths.

The band edges of $GaP_{1-x}N_x$/GaP($x$ = 0–0.035) were previously reported to be negative by more than 300 mV.[28] This might be associated with the structures of thin films grown in mismatch between the $GaP_{1-x}N_x$ film and substrate GaP. The flat band potentials of GaP at pH = 0 are in the range of 1.2–0.93 V,[39] and thus the band edge for the oxidation of water is negative or very slightly positive, which makes it difficult for water splitting to proceed efficiently. On the other hand, ZnO/GaN has a valence band level considerably lower than the water oxidation level. The valence bands of ZnO/GaN-P consist of the hybridized Ga 4p + P 3p + N 2p AOs, which forms intermediate electronic band structures of GaP and GaN. Thus, the N atom inclusion to GaP lowers the valence band edge enough for the oxidation to proceed. This has positive effects on the oxidation of water, although the conduction band edge shifts to a lower energy level. The disadvantage of not only GaP but possibly many metal

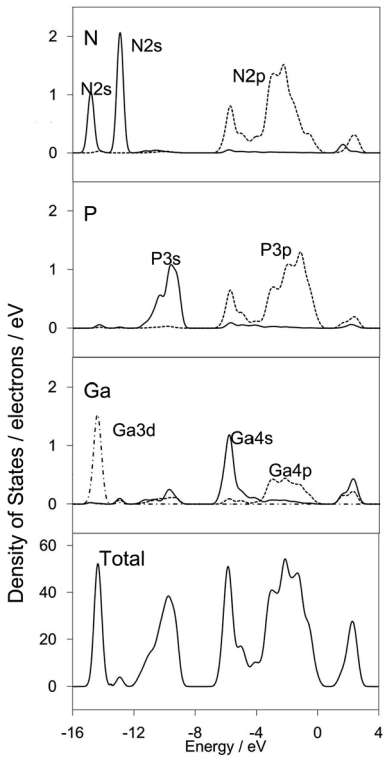


Fig. 10 Density of states for a $Ga_{32}P_{32}N_1$ model cluster. In AO-PDOS of N, P and Ga atoms, solid line (—) is for s orbital, dash line (— — — —) for p orbital, and alternate long and short dash line(— - — -) for d orbital. Total DOS is shown with a solid line.

 

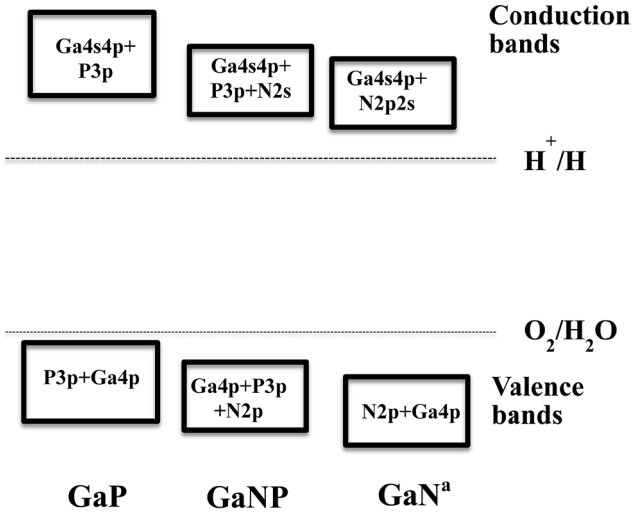


Fig. 11 Schematic band structures and energy levels of GaP, GaNP and GaN. [a]Indicates result from ref. 1.

phosphides is the valence band edge being higher than or nearly the same as the oxidation level of water. Schematic band structures and energy levels are schematically depicted in Fig. 11. The presented results indicate that the consolidation of metal phosphides with N atoms is able to extend the availability of meal phosphides to photocatalysts for water splitting.

In conclusion, the phosphidation of active ZnO/GaN photocatalysts significantly enhances the photocatalytic activity for water splitting. The phosphidation of ZnO/GaN successfully permits to achieve optimal nitrogen conditions in $GaP_{1-x}N_x$, which leads to the generation of high photocatalytic performance. The present approach shows promise for application to other metal nitride systems that will be advantageous for efficient photocatalysts for water splitting.

## Acknowledgements

Financial support from INPEX is gratefully appreciated.

## References

1 N. Arai, N. Saito, H. Nishiyama, K. Domen, H. Kobayashi, K. Sato and Y. Inoue, *Catal. Today*, 2007, **129**, 407–413.
2 N. Arai, N. Saito, H. Nishiyama, Y. Inoue, K. Domen and K. Sato, *Chem. Lett.*, 2006, **35**, 796–797.
3 K. Maeda, T. Takata, M. Hara, N. Saito, Y. Inoue, H. Kobayashi and K. Domen, *J. Am. Chem. Soc.*, 2005, **127**, 4150–4151.
4 K. Teramura, K. Maeda, T. Saito, T. Takata, N. Saito, Y. Inoue and K. Domen, *J. Phys. Chem. B*, 2005, **109**, 21915–21921.
5 K. Maeda, K. Teramura, T. Takata, M. Hara, N. Saito, K. Toda, Y. Inoue, H. Kobayashi and K. Domen, *J. Phys. Chem. B*, 2005, **109**, 20504–20510.
6 K. Maeda, K. Teramura, D. Lu, T. Takata, M. Hara, N. Saito, Y. Inoue and K. Domen, *Nature*, 2006, **440**, 295.
7 K. Maeda, K. Teramura, H. Masuda, T. Takata, N. Saito, Y. Inoue and K. Domen, *J. Phys. Chem. B*, 2006, **110**, 13107–13112.
8 K. Maeda, K. Teramura, N. Saito, Y. Inoue and K. Domen, *J. Catal.*, 2006, **243**, 303–308.
9 K. Maeda, K. Teramura, D. Lu, N. Saito, Y. Inoue and K. Domen, *J. Phys. Chem. C*, 2007, **111**, 7554–7560.
10 M. Yoshida, T. Hirai, K. Maeda, N. Saito, J. Kubota, H. Kobayashi, Y. Inoue and K. Domen, *J. Phys. Chem. C*, 2010, **114**, 15510–15515.
11 J. R. Chelikowsky and M. L. Cohen, *Phys. Rev. B*, 1976, **14**, 556–582.
12 C. S. Wang and B. M. Klein, *Phys. Rev. B*, 1981, **24**, 3393–3416.
13 D. G. Thomas and J. J. Hopfield, *Phys. Rev.*, 1966, **150**, 680–689.
14 E. Cohen and M. D. Sturge, *Phys. Rev. B*, 1977, **15**, 1039–1051.
15 S. Miyoshi, H. Yaguchi, K. Onabe, R. Ito and Y. Shiraki, *Appl. Phys. Lett.*, 1993, **63**, 3506–3508.
16 H. Yaguchi, S. Miyoshi, G. Biwa, M. Kibune, K. Onabe, Y. Shiraki and R. Ito, *J. Cryst. Growth*, 1997, **170**, 353–356.
17 Y. Zhang, B. Fluegel, A. Mascarenhas, H. P. Xin and C. W. Tu, *Phys. Rev. B*, 2000, **62**, 4493–4500.
18 W. Shan, W. Walukiewicz, K. M. Yu, J. Wu, J. W. Ager III, E. E. Haller, H. P. Xin and C. W. Tu, *Appl. Phys. Lett.*, 2000, **76**, 3251–3253.
19 H. P. Xin, C. W. Tu, Y. Zhang and A. Mascarenhas, *Appl. Phys. Lett.*, 2000, **76**, 1267–1269.
20 G. Y. Rudko, I. A. Buyanova, W. M. Chen, H. P. Xin and C. W. Tu, *Appl. Phys. Lett.*, 2002, **81**, 3984–3986.
21 C. V. Reddy, R. E. Martinez II, V. Narayanamurti, H. P. Xin and C. W. Tu, *Phys. Rev. B*, 2002, **66**, 235313-1–235313-4.
22 J. N. Baillargeon, K. Y. Cheng, G. E. Hofler, P. J. Pearah and K. C. Hsieh, *Appl. Phys. Lett.*, 1992, **60**, 2540–2542.
23 R. A. Faulkner and P. J. Dean, *J. Lumin.*, 1970, **1–2**, 552–561.
24 B. Gil, J. P. Albert, J. Camassel, H. Mathieu and B. C. Guillaume, *Phys. Rev. B*, 1986, **33**, 2701–2712.
25 L. Bellaiche, Su-H. Wei and A. Zunger, *Phys. Rev. B*, 1997, **56**, 10233–10240.
26 P. R. C. Kent and A. Zunger, *Phys. Rev. Lett.*, 2001, **86**, 2613–2616.
27 P. R. C. Kent and A. Zunger, *Phys. Rev. B*, 2001, **64**, 115208-1–115208-23.
28 T. G. Deutsch, C. A. Koval and J. A. Turner, *J. Phys. Chem. B*, 2006, **110**, 25297–25307.
29 M. C. Payne, M. P. Teter, D. C. Allan, T. A. Arias and J. D. Johannopoulos, *Rev. Mod. Phys.*, 1992, **64**, 1045–1097.
30 D. Vanderbilt, *Phys. Rev. B*, 1990, **41**, 7892–7895.
31 S. J. Clark, M. D. Segall, C. J. Pickard, P. J. Hasnip, M. I. J. Probert, K. Refson and M. C. Payne, *Z. Kristall*, 2005, **220**, 567–570.
32 J. P. Perdew and A. Zunger, *Phys. Rev. B*, 1981, **23**, 5048–5079.
33 J. P. Perdew, *Phys. Rev. B*, 1986, **33**, 8822–8824.
34 A. D. Becke, *Phys. Rev. A*, 1988, **38**, 3098–3100.
35 H. J. Monkhorst and J. D. Pack, *Phys. Rev. B*, 1976, **13**, 5188–5192.
36 A. J. C. Wilson, *Mathematical Theory of X-ray Powder Diffraction*, Philips Technical Library, Eindhoven, 1963.
37 G. B. Stringfellow, *J. Electrochem. Soc.*, 1972, **119**, 1780–1782.
38 L. L. Jensen, J. T. Muckerman and M. D. Newton, *J. Phys. Chem. C*, 2008, **112**, 3439–3446.
39 G. Horowitz, *J. Appl. Phys.*, 1978, **49**, 3571–3573.